
Effect of Ice and Hydrate Formation on Thermal Conductivity of Sediments

Evgeny Chuvilin, Boris Bukhanov, Viktor Cheverev,
Rimma Motenko and Erika Grechishcheva

Additional information is available at the end of the chapter

<http://dx.doi.org/10.5772/intechopen.75383>

Abstract

Thermal conductivity of ice- and hydrate-bearing fine-grained porous sediments (soils) has multiple controls: mineralogy, particle size, and physical properties of soil matrix; type, saturation, thermal state, and salinity of pore fluids; and pressure and temperature. Experiments show that sediments generally increase in thermal conductivity upon freezing. The increase is primarily due to fourfold difference between thermal conductivity of ice and water (~ 2.23 against ~ 0.6 W/(m·K)) and is controlled by physicochemical processes in freezing sediments. Thermal conductivity of frozen soils mainly depends on lithology, salinity, organic matter content, and absolute negative temperature, which affect the amount of residual liquid phase (unfrozen water). It commonly decreases as soil contains more unfrozen water, in the fining series 'fine sand – silty sand – sandy clay – clay', as well as at increasing temperatures, salinity, or organic carbon contents. According to experimental evidence, the behavior of thermal conductivity in hydrate-bearing sediments strongly depends on conditions of pore hydrate formation. It is higher when pore hydrates form at positive temperatures ($t > 0^\circ\text{C}$) than in the case of hydrate formation in frozen samples. Freezing and thawing of hydrate-bearing sediments above the equilibrium pressure reduces their thermal conductivity due to additional hydrate formation.

Keywords: thermal conductivity, sediments, temperature, ice, gas hydrate, freezing, permafrost, unfrozen water, salinity, hydrate saturation, organic matter

1. Introduction

Thermal conductivity of rocks depends on their origin and deposition environments and related lithology, mineralogy, structure and texture, as well as on thermal state and

thermodynamic conditions [1–13]. There is a wealth of published evidence on thermal conductivity control by mineralogy, particle size, pore space structure, and pore fluid state and composition: whether it is fresh or saline water, ice, gas, organic compounds, and so on [14–21]. However, the effect of some pore filling materials on thermal properties of sediments remains poorly investigated, especially that of pore hydrates [22, 23]. Natural gas hydrates share much physical similarity with ice (heat capacity, density, and acoustic properties) and thus pore hydrates in permafrost, though being known since the 1970s [24], are hard to identify and study with conventional geophysical methods, mainly seismic. Meanwhile, pore gas hydrate and ice differ markedly in thermal conductivity, which is 2.23 W/(m·K) in hydrate, 0.54–0.65 W/(m·K) in ice, and 0.6 W/(m·K) in liquid water [25–27].

Knowledge of thermal properties, especially thermal conductivity, of frozen and freezing porous sediments is valuable in geocryological predictions for reducing geological engineering risks during construction and operation of buildings and utilities in regions of Arctic and highland permafrost [28, 29]. True thermal conductivity values of frozen soils are also indispensable to choose optimal strategies of mitigating risks from permafrost thawing as a result of global warming or local manmade impacts.

The development of hydrate-bearing gas and oil reservoirs likewise requires knowing their thermal properties [30]. Methane production from these reservoirs is most often simulated with reference to thermal conductivity of pure methane hydrates [31], but this simplistic assumption can entrain serious errors during methane recovery, especially for permafrost containing hydrates and ice.

The marked thermal conductivity difference between hydrate and ice is a prerequisite for creating a method of identifying and mapping intra-permafrost gas hydrates.

2. Thermal conductivity of sediments in unfrozen and frozen state and freezing effect

Thermal properties of rocks, soils, water, and air vary as a function of their composition, structure and state, as well as thermodynamic conditions. Thermal conductivity values of different materials are quoted in **Table 1** per unit volume of rocks, sediments, water, ice, snow and air. Note that it linearly depends on temperature for water, ice and air.

Comparative analysis of experimental data shows that thermal conductivity of igneous (granite, basalt), metamorphic (quartzite, schists), and sedimentary (sandstone, limestone, dolomite) rocks can vary from 1.0 to 5.0 W/(m·K) as a function of different factors. The mineralogy dependence is associated with the presence of thermally conductive minerals, such as SiO₂ quartz (~7.0 W/(m·K)) or iron-bearing phases (e.g., pyrite). Density and porosity effects appear as greater thermal conductivity in denser and less porous rocks, that is, it is lower in sediments than in igneous or metamorphic rocks. Experiments show that 15–20% densening of skeleton in sand leads to about twice higher thermal conductivity. The variations result from more or less close packing of particles. Manmade compaction likewise leads to thermal conductivity increase in sediments, which is often used in civil engineering.

Cemented porous sediments fall into three thermal conductivity groups: (1) coarse clastics (conglomerates, gritstones, and sandstones); (2) fine clastics (silt and clay); (3) chemogenic and biogenic carbonates and silicates (dolomite, anhydrite, limestone, diatomite, etc.). Thermal conductivity of coarse clastics is from 1.5 to 4.5 W/(m·K), estimated separately for matrix and cement, and reaches 5.8 W/(m·K) in low-porosity monomineral sediments (dolomite, limestone). Thermal conductivity is anisotropic in many sedimentary and metamorphic rocks: it is on average 10–30% higher along than across the bedding, especially in shale and gneiss [32]. The reason is that interactions of mineral particles and heat transfer are more active along the bedding controlled by the origin and deposition environments of rocks.

Thermal conductivity variations in sediments and soils, which are multicomponent and multiphase systems, depend on relative percentages of solid, liquid, and gas phases; soil chemistry and mineralogy; structure and texture (particle size, porosity, layering, etc.); moisture contents; and temperature. Saturation of sediments affects significantly their thermal properties: thermal conductivity reaches its maximum at full water saturation [11] as water with $\lambda = 0.54$ (W/(m·K)) supplants gas with $\lambda = 0.024$ (W/(m·K)).

The dependence on particle size composition shows up in higher thermal conductivity of coarse and very coarse soils (of boulder, pebble, gravel, and sand particles) compared to finer-grained varieties, the moisture content, density, and other parameters being equal. The upper limit for coarse sediments (up to 3–9 W/(m·K)) corresponds to hard components while the lower limit (0.3–0.5 W/(m·K)) represents dry fine-grained material. Thermal conductivity decreases with fining, in a descending series of sand – silt – clay – peat (**Table 1**), because of a greater number of loose contacts between particles [33].

Saturated frozen sediments and soils with medium or high moisture contents have higher thermal conductivity than their unfrozen counterparts because pore ice is four times more conductive than water (**Table 1**): 2.22 W/(m·K) against 0.54 W/(m·K). However, the temperature dependence of thermal conductivity in wet porous sediments is rather controlled by relative percentages of pore ice and water and conditions of heat transfer at their contacts. Within the range of positive temperatures, thermal conductivity decreases slowly from 25 to 0°C, in accordance with linear dependence on water temperature, but rises abruptly at the transition from 0 to -1°C when pore water rapidly converts to ice (**Figure 1**). Note that thermal conductivity of ice-rich soil depends more on the conditions of cooling and heating than on absolute temperature. Of special importance is the direction of heat transfer at alternating pressures and temperatures, when pore water converts to ice and back, and changes in their relative amounts [15]. **Figure 2** shows qualitative variations of thermal conductivity in frozen sediments subject to further freezing and subsequent thawing. The curves comprise several segments corresponding to different temperature intervals. Thermal conductivity decreases linearly within the range of positive temperatures till the onset of freezing (segment A-B) and then increases dramatically in the region of rapid water-to-ice transition (segment B-C), when ice, with its thermal conductivity four times that of water, appears as a new pore filling component, while the amount of unfrozen pore water reduces. Further freezing to -15°C and colder (segment C-D) corresponds to notable (30–40%) decrease in thermal conductivity. The reason is that increasing crystallization of unfrozen bound water and related thermomechanic stress, as well as thermal expansion variations, cause rapid growth of cracks. Saline

Material	Thermal conductivity λ (W/(m·K))
Water	
At +4.1°C	0.54
At +20°C	0.60
Ice	2.22–2.35
Air	
At 0°C	0.024
At –23°C	0.022
Snow	
Loose	0.1
Dense	0.3–0.4
Granite	2.3–4.1
Basalt	1.74–2.91
Quartzite	2.9–6.4
Shale	1.74–2.33
Sandstone	0.7–5.8
Limestone	0.8–4.1
Dolomite	1.1–5.2
Sand	
Dry	0.3–0.35
Unfrozen, water-saturated	1.7–2.6
Frozen, ice-saturated	1.5–3.0
Silty clay	
Dry	0.19–0.22
Unfrozen, water-saturated	0.6–1.0
Frozen, ice-saturated	1.2–1.4
Clay	
Air-dry	0.8–1.0
Unfrozen, water-saturated	1.2–1.4
Frozen, ice-saturated	1.4–1.8
Peat	
Dry	0.012–0.14
Unfrozen, water-saturated	0.7–0.9
Frozen, ice-saturated	1.1–1.2

Table 1. Thermal conductivity of different materials [19].

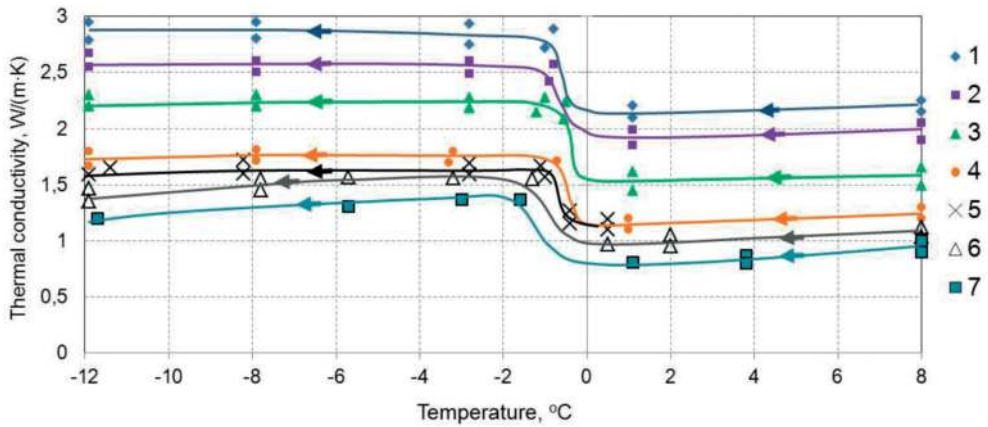


Figure 1. Effect of temperature on thermal conductivity in different types of sediments: 1—coarse crushed stone filled with silt, 2—fine sand, 3—silty sand, 4—loess-like silty clay, 5—silty clay, 6—clay, and 7—degraded peat [15, 19]. Data points are experimental measurements; lines are approximation trends. The arrows show the direction of temperature change.

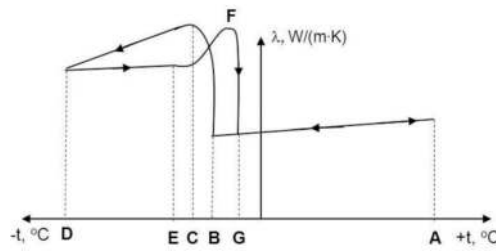


Figure 2. Variations of thermal conductivity in frozen sediments subject to freezing and subsequent thawing. The arrows show the direction of temperature change.

peat-bearing fine-grained porous soil contains much unfrozen water even at low negative temperatures, till -15°C [16, 19, 34]. The thermal conductivity reduction is especially large in ice-rich peat subject to further cooling and related brittle deformation when internal stress in soil releases through microcracks.

Subsequent warming (segment E-F) leads to notable increase in thermal conductivity as the cracks heal up because ice, and soil as a whole, become more plastic. The highest thermal conductivity values in the warming-thawing cycle of frozen soil approach those in the freezing-cooling cycle, but correspond to higher negative temperatures because of hysteretic behavior of moisture phases. Thermal conductivity decreases dramatically till the thawing temperature within the segment F-G, as pore ice melting increases the contents of liquid water.

The thermal conductivity decreases with grain sizes in the series ‘coarse sand – fine sand – silty sand – silt – silty clay – clay’ was observed in both frozen and unfrozen sediments with

different degrees of water or ice saturation [15, 17–21], over the range of temperatures from +20 to -20 °C, including the region of rapid water-ice phase transitions. Finer sediments have more thermal resistance contacts and are more hydrophilic and ultraporous, which increases relative contents of low-conductive liquid unfrozen water.

Thermal conductivity of frozen sediments increases systematically with ice saturation as low-conductivity gas gives way to high-conductivity ice. Sediments with high contents of ice, which swells out the mineral skeleton, have thermal conductivity about that of ice.

Salinity, or the presence of soluble salts in pore water, is another important control of thermal conductivity in frozen sediments. Namely, Na⁺ and Cl⁻ ions lead to changes in the phase state of pore moisture in permafrost. Frozen soils with higher salinity (Z, %), that is, salt-to-dry sediment weight ratio, contain more unfrozen pore water and, correspondingly, have lower thermal conductivity (**Figure 3**). Thermal conductivity of saline sand and silty sand containing liquid pore water is much lower than that in non-saline sediments: only 1% increase of salinity in frozen sand may cause twofold thermal conductivity decrease. Unlike sand, more or less water-saturated low saline (0 to 0.5–0.7%) clay silt and clay have thermal conductivity slightly (within 10%) higher than in their non-saline counterparts, but more saline varieties are less conductive. Namely, at Z > 1%, thermal conductivity shows a weak decreasing trend traceable until the system reaches the eutectic point. This behavior is related primarily with changes in relative contents of water phases (ratio of unfrozen water content to total moisture content) as salinity increases. The amount of liquid water depends on concentration as well as on chemistry of salts: it increases progressively in the series Na₂SO₄-Na₂CO₃-NaNO₃-NaCl, while thermal conductivity decreases correspondingly. Note that further cooling of frozen soils reduces the amount of unfrozen pore water [34]. As the pore fluid reaches eutectic concentration and temperature, salts form cryohydrates, whereby the content of unfrozen water decreases dramatically. The formation of thermally conductive cryohydrates in the pore space and the respective reduction of the liquid water content leads to thermal conductivity increase in frozen soils. Experiments show that thermal conductivity of saline soils tends to that of non-saline soils at temperatures below eutectics [35].

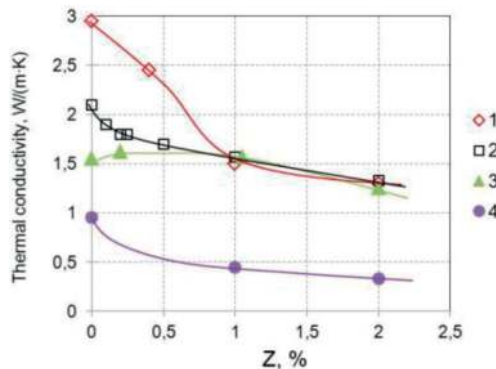


Figure 3. Salinity (Z,%) dependence of thermal conductivity for different types of NaCl-bearing soil: 1—fine sand, 2—silty sand, 3—sandy clay, and 4—kaolin clay ($W = 15\text{--}30\%$ for 1–3 and $W = 50\text{--}70\%$ for 4) [18]. Data points are experimental measurements; lines are approximation trends.

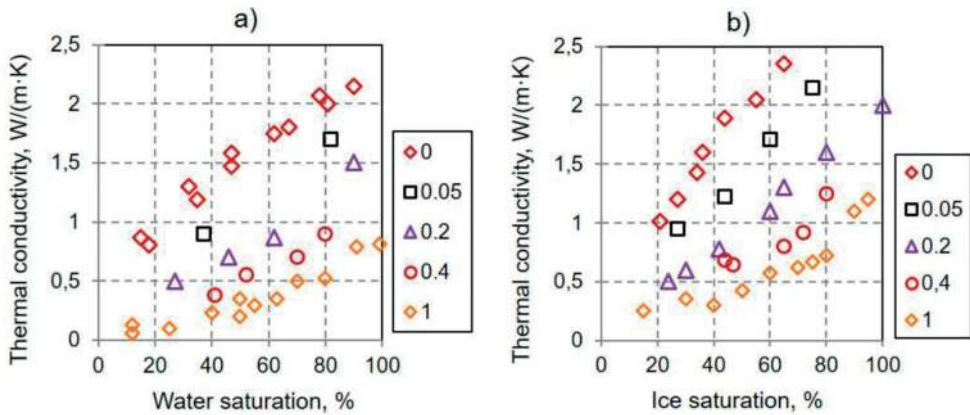


Figure 4. Water (a) and ice (b) saturation dependence of thermal conductivity in unfrozen and frozen peat-bearing sandy soils with different peat contents [36] (found as organic component to total sediment dry weight ratio).

Thermal conductivity is lower in frozen sediments containing organic matter (especially, peat) (Figure 4). This is because the presence of peat increases specific surface activity and the contents of unfrozen pore water, and the organic component itself (peat, oil, etc.) most often has lower thermal conductivity than mineral particles and ice. Therefore, unfrozen water-saturated soils with organic-filled porosity likewise have low thermal conductivity.

Unlike heat capacity, thermal conductivity is not an additive value but depends on sediment structure and texture. As shown by experiments, massive frozen clay is more conductive than that with ice lenses at similar water contents and density. Note that thermal conductivity of sediments with lenticular cryostructure is anisotropic: it is 20–30% higher at heat flux along than across ice lenses. The reason is in higher thermal conductivity of ice and lower thermal resistance at contacts between mineral layers and ice lenses.

3. Thermal conductivity of gas hydrate-bearing sediments and hydrate-accumulation effect

Thermal conductivity has been worse studied in hydrate-bearing sediments than in frozen (ice-bearing) sediments: the available data are limited to sporadic estimates for manmade hydrate-bearing materials [37–41]. The first experimental evidence on thermal conductivity of sediments containing natural gas hydrates was obtained from well Malik 5L-38 (Mackenzie Delta, Canada). Ice-bearing soils were found to have thermal conductivity generally higher than their hydrate-bearing counterparts [42]. On the other hand, frozen hydrate-saturated sediments are often more thermally conductive than those in the unfrozen state. New experimental data on thermal conductivity of natural gas hydrate-bearing sediments from the Nankai Trough published a few years ago were used to predict thermal conductivity from the known particle size distribution, porosity, and hydrate saturation [43]. The most successful prediction for natural sediments with hydrate saturation within 14% was achieved with a model of

complex distribution (geometric mean), but the proposed equations were poorly applicable to sediment samples containing greater percentages of hydrates (up to 30%) [44]. This is because hydrate-bearing sediments are actually complex systems and their thermal conductivity is not a sum of values for the system constituents but rather depends on the pore space structure.

According to experimental evidence, hydrate formation conditions influence largely the thermal conductivity of hydrate-bearing sediments [45]. Its variations were studied at different conditions of hydrate formation: (1) low positive temperatures ($t \approx +2 \pm 1^\circ\text{C}$), (2) negative temperatures ($t \approx -5 \pm 1^\circ\text{C}$), (3) cooling from $+2 \pm 1$ to -5 and -8°C , where residual pore water (not converted to hydrate at positive temperatures) froze and induced additional hydrate formation, and (4) warming from -5 ± 1 to $+2 \pm 1^\circ\text{C}$, where residual pore ice (not converted to hydrate at negative temperatures) thawed and induced additional hydrate formation.

3.1. Hydrate formation at $t > 0^\circ\text{C}$

First, the effect of gas hydrate formation at $t > 0^\circ\text{C}$ on thermal conductivity of hydrate-bearing sediments was studied at low positive temperatures ($t = +2 \pm 1^\circ\text{C}$). The typical pattern of pore hydrate formation, under favorable conditions, is evident in time-dependent variations in the fraction of pore space occupied by hydrates or hydrate saturation (S_{hr} , %) (Figure 5). This fraction decreases with time as a result of changes in the hydrate formation mechanism. Hydrate formation is rapid early during the process, and most of hydrate forms within the first 45–50 h, while S_{hr} (Figure 5) reaches 67%. Then hydrate formation decelerates, while S_{hr} remains almost invariable (about 67%). The observed kinetics of hydrate formation at low positive temperatures can be explained as follows. Rapid formation of hydrates in the beginning is due to direct gas-water contacts. Later, a gas hydrate film forms at the pore water-gas interface and impedes gas access to pore water, whereby the hydrate formation rate slows down, being limited by the permeability of the gas hydrate film. The thickening of the hydrate film makes it much less permeable, and hydrate formation almost stops at a certain film thickness, despite the fact that the residual pore water content exceeds its equilibrium content at the given temperatures and pressures.

The time-dependent behavior of thermal conductivity during hydrate accumulation in gas-saturated silty sand ($W = 18\%$) at positive temperatures is irregular (Figure 6). The curve

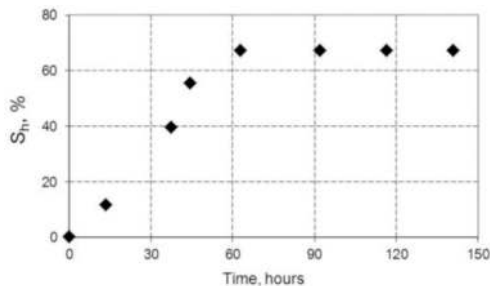


Figure 5. Pore hydrate formation in gas-saturated silty sand ($W = 18\%$; $n = 0.40$), at $t = +2 \pm 1^\circ\text{C}$: time-dependent hydrate saturation (S_{hr} , %) [45].

comprises three characteristic segments: (1) thermal conductivity (λ) changes little (1.77–1.78 W/(m·K) or within a measurement accuracy of 3%) for the first 40 h, but (2) becomes 13% higher (1.78–2.01 W/(m·K)) for the following 20 h, and (3) remains almost invariable about 2.01 W/(m·K), with 3–4% variations (within a measurement accuracy) till 60 h after the run start. While thermal conductivity almost does not change for the first 40 h, saturation (S_h) becomes 40% higher than at the run onset; then both parameters increase for the following 20 h, peak concurrently, and remain invariable within 100 h afterward.

At gas saturation S_h within 45%, thermal conductivity does not change (**Figure 7**), as reported previously [42–44]. The variations become notable when hydrates occupy more than 45% of the pore space. For instance, thermal conductivity became 14% higher, while S_h reached 61% in silty sand ($W = 18\%$) and 9% higher as S_h increased to 57% in fine sand.

3.2. Hydrate formation at $t < 0^\circ\text{C}$

Hydrate formation at $t < 0^\circ\text{C}$ was studied in frozen methane-bearing samples in a pressure cell, at temperatures of $-5 \pm 1^\circ\text{C}$ (**Figure 8**). Unlike the tests at low positive temperatures, methane hydrates form more slowly at negative temperatures. As a result, the rate of hydrate formation in frozen samples is commensurate with that at positive temperatures for quite a long time. The reason is that, at negative temperatures, gas hydrates form directly on the surface of ice particles, as demonstrated by special studies of interaction between ice particles and CO_2 and CH_4 gases [46, 47]. Hydrate that forms during this interaction has a low density, and, hence, a high permeability and does not impede much the conversion of ice particles to hydrate. The same mechanism apparently works during transition of pore ice into hydrate, judging by the dynamics of gas hydrate formation in frozen sediments. Unlike the case of $t > 0^\circ\text{C}$, the thermal conductivity of frozen samples decreases nonuniformly with time during hydrate formation (**Figure 9**). The decrease is to 1.81 W/(m·K) (8%) for the first 50 h of hydrate growth and then as small as 3% for the subsequent 125 h. In general, this decrease is observed in the S_h range from 0 to 50–60% (**Figure 10**). The thermal conductivity decrease most likely results from reduction in the amount of ice, with its thermal conductivity as high as 2.23 W/(m·K), and the related growth in the share of the less conductive hydrate (0.6 W/(m·K)).

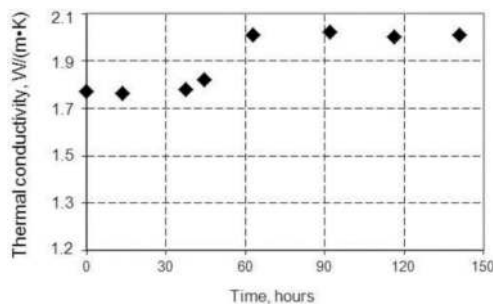


Figure 6. Time-dependent thermal conductivity of gas-saturated silty sand ($W = 18\%$; $n = 0.40$) during hydrate formation at $t = +2 \pm 1^\circ\text{C}$ [45].

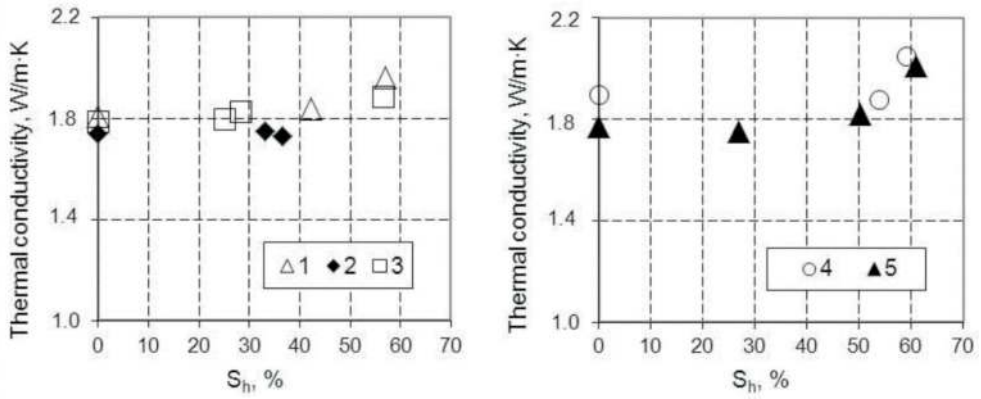


Figure 7. Thermal conductivity of sediments as a function of hydrate saturation (S_{hr} , %) at $t = +2 \pm 1^\circ\text{C}$: (1) fine sand, $W = 16\%$; (2) fine sand, $W = 10\%$; (3) fine sand, $W = 15\%$; (4) fine sand +14% kaolin clay, $W = 15\%$; and (5) silty sand, $W = 18\%$ [45].

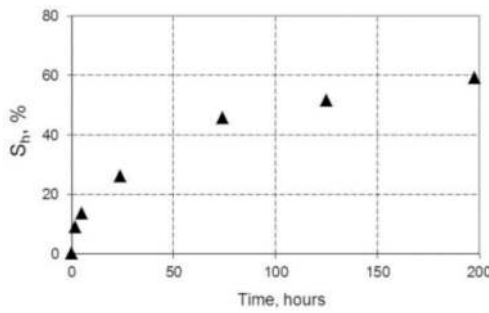


Figure 8. Pore methane hydrate formation in frozen fine sand ($W = 22\%$; $n = 0.60$) at $t = -5 \pm 1^\circ\text{C}$: time-dependent hydrate saturation (S_{hr} , %) [45].

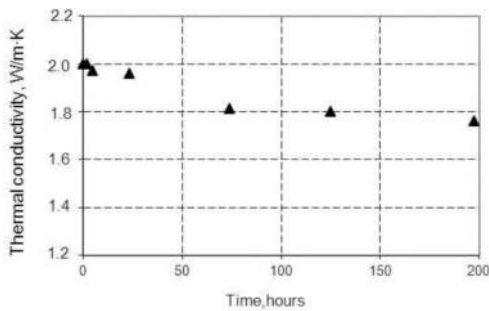


Figure 9. Time-dependent thermal conductivity of gas-saturated fine sand ($W = 22\%$; $n = 0.60$) during hydrate formation at $t = -5 \pm 1^\circ\text{C}$ [45].

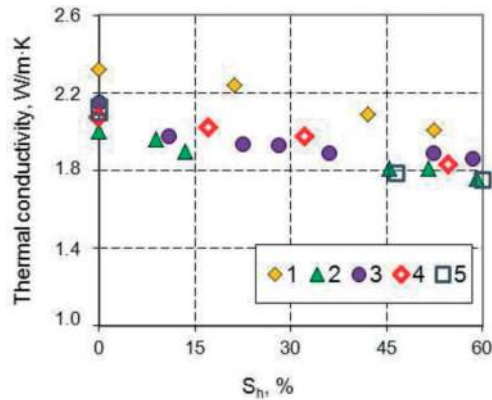


Figure 10. Thermal conductivity of sediments as a function of hydrate saturation (S_h , %), at $t = -5 \pm 1^\circ\text{C}$: (1) fine sand, $W = 19\%$ and $n = 0.40$; (2) fine sand, $W = 22\%$ and $n = 0.60$; (3) fine sand, $W = 15\%$ and $n = 0.38$; (4) silty sand, $W = 24\%$ and $n = 0.60$; and (5) silty sand, $W = 16\%$ and $n = 0.38$ [45].

3.3. Effect of freezing

To study the effects of freezing on thermal conductivity, the samples saturated with hydrate at $t > 0^\circ\text{C}$ were cooled from -5 to -8°C . Although hydrate had already saturated 50–60% of the pore space before freezing and the hydrate formation almost ceased, the samples produced additional pore hydrate upon further cooling, in all runs (**Table 2**), more in silty sand than in fine sand. Thus, a large portion of residual water that survived conversion to hydrate at positive temperatures became consumed during cooling and freezing. Hydrate formation became more active as the survived pore water froze up because cryogenic deformation of the soil skeleton and release of dissolved gas produced new water-gas interfaces. The amount of hydrate additionally formed as a result of freezing mainly depends upon soil mineralogy, clay content, and water saturation.

Thermal conductivity decreased dramatically in freezing hydrate-saturated sediments (**Figure 11 A**) but became 15–20% higher in hydrate-barren samples (**Figure 11 B**). The freezing-induced thermal conductivity reduction was 10% in fine sand (from 1.96 to 1.77 W/(m·K)) but reached 50% in silty sand with $W = 16\%$ (2.01–0.96 W/(m·K)) [45].

Type of soil	W (%)	S_h (%)	
		Before freezing	After freezing
Fine sand	16	58	71
Fine sand +14% kaolin	15	62	79
Silty sand	18	61	85
Silty sand	16	52	79

Table 2. Methane hydrate formation upon freezing of residual pore water [45].

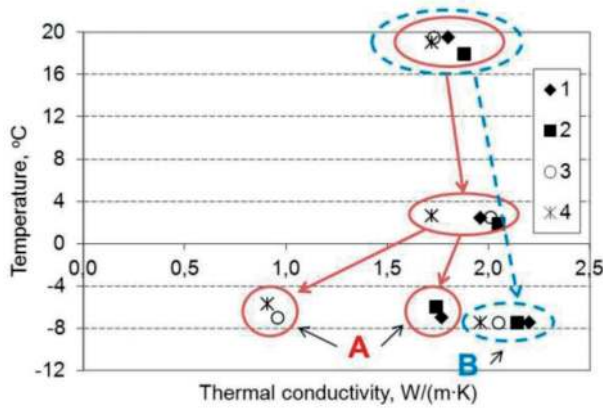


Figure 11. Variations in thermal conductivity of gas-saturated sediments upon cooling (to +2°C) and freezing: (A) hydrate-bearing samples after freezing and (B) frozen hydrate-barren samples. Solid (red) and dash (blue) lines correspond to samples saturated with gases that can and cannot form hydrates (methane and nitrogen, respectively): (1) fine sand, $W = 16\%$; (2) fine sand +14% kaolin, $W = 15\%$; (3) silty sand, $W = 18\%$; and (4) silty sand, $W = 16\%$.

Thus, thermal conductivity may decrease dramatically in hydrate-saturated sediments exposed to further freezing, whereby the survived pore water freezes up, as a result of additional hydrate formation. This behavior may be due to structure and texture changes in freezing gas- and hydrate-bearing sediments. These are especially the effects of heaving or cracking of hydrate-saturated soil or the formation of highly porous hydrate at grain boundaries, with thermal conductivity as low as ~ 0.35 W/(m·K).

3.4. Effect of thawing

To study the effect of thawing on the behavior of thermal conductivity, the frozen sand samples that were saturated with hydrate at $t < 0^\circ\text{C}$ were heated to $+2 \pm 1^\circ\text{C}$. The tests showed additional hydrate formation in fine sand (Table 3), as in the case of freezing, but unlike the latter case, it did not exceed 10% [45]. Faster hydrate generation upon thawing was attributed to deformation of soil skeleton and formation of new water-gas interfaces. Additional hydrate formation upon thawing of hydrate-saturated sand was more intense in the initially water-saturated samples: 10 and 7% of additional hydrate formed in sandy samples with $W = 19$ and 15%, respectively. As the frozen hydrate-bearing samples thawed, their thermal conductivity

Type of sediment	W (%)	S_h (%)	Thermal conductivity (W/(m·K))	
			Before thawing	After thawing
Fine sand	19	0.64	0.71	1.80
Fine sand	15	0.57	0.61	1.86

Table 3. Thermal conductivity and hydrate saturation of frozen hydrate-bearing sand upon thawing (to $+2 \pm 1^\circ\text{C}$) at above-equilibrium methane pressure [45].

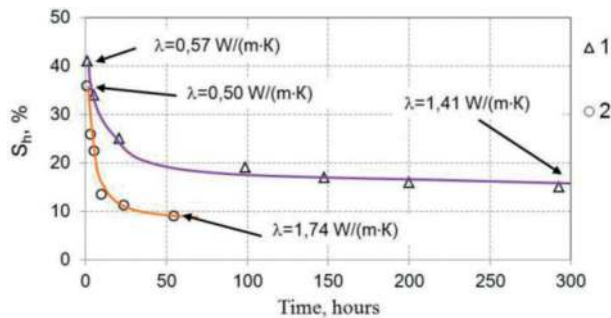


Figure 12. Thermal conductivity variations of frozen hydrate-contain sands during methane hydrate dissociations at $t = -5$ to -6°C and pressure 0.1 MPa: Data points (triangles and circles) are experimental measurements; lines are approximation trends: (1) fine sand, $W = 17\%$ and $n = 0.40$; (2) silty sand, $W = 17\%$ and $n = 0.40$.

decreased (from 1.86 to 1.72 W/(m·K) or for 8%). Two main reasons of such reduction are (1) thermal conductivity difference between pore ice and water and (2) hydrate saturation increase. Thus, both freezing and thawing cause thermal conductivity reduction in frozen soils saturated with methane hydrate at above-equilibrium pressures.

The observed thermal conductivity variations associated with hydrate formation at different conditions (low positive and negative temperatures, freezing and thawing) indicate that this behavior is mostly controlled by phase transitions in pore fluids and by structure and texture changes in main sample constituents, which were explained by Chuvilin and Bukhanov [45] in two models of structure and texture changes in gas-saturated sediment during hydrate formation. These models can be used for reference in geomechanical and thermal simulations of gas hydrate reservoirs, taking into account the conditions of pore hydrate formation, with implications for methane recovery.

3.5. Effect of hydrate dissociation

The effect of hydrate dissociation on thermal conductivity of frozen hydrate-bearing soils at below-equilibrium pressure was investigated in manmade sand samples at temperatures about -5 to -6°C and atmospheric pressure [48]. Pore hydrates in the frozen sand samples failed to reach complete decomposition in the experiments due to their self-preservation [49–52], with residual hydrate saturation (S_h , %) up to 10% or more (Figure 12). The hydrate dissociation was attendant with notable increase in thermal conductivity; it became 2.5 times higher (from 0.57 W/(m·K) to 1.41 W/(m·K) as S_h reduced from 40 to 15%) in fine sand and more than three times higher as S_h became 10% in silty sand. Thermal conductivity increase in the end of the experiment was due to decrease in the amount of pore hydrate and increase in pore ice, with residual hydrate saturation (S_h , %) of 10% (Figure 11). Low thermal conductivity of frozen hydrate-bearing samples (0.5–0.6 W/(m·K)) for first few minutes after the equilibrium pressure drop to the atmospheric value (0.1 MPa) may result from both high contents of pore hydrate and formation of microcracks in this hydrate which heal up afterward during its dissociation [53].

4. Conclusions

Thermal conductivity of wet porous fine-grained soils depends on particle size, mineralogy, pore space structure, and moisture contents, as well as on the phase state and phase change of pore fluids. The effects of water→ice, water→gas hydrate, and ice→gas hydrate transitions were studied in experiments, which show the phase change direction and relative contents of water phases in the pore space to be principal controls of thermal conductivity. It increases in wet porous sediments subject to freezing and subsequent cooling, primarily, due to pore water-to-ice conversion at a wide range of negative temperatures. However, the process may induce microcracking, which may reduce thermal conductivity.

Thermal conductivity of frozen sediments mainly depends on lithology, salinity, organic matter content, and absolute negative temperature, which affect the amount of residual liquid phase (unfrozen water) in frozen soils. Namely, thermal conductivity commonly decreases as soil contains more unfrozen water, in the series 'fine sand – silty sand – sandy clay – clay', as well as at increasing salinity or organic (e.g., peat) contents.

As demonstrated by our experiments, thermal conductivity can either increase or decrease depending on hydrate formation conditions. Namely, it increases if gas hydrates form at positive temperatures ($t > 0^{\circ}\text{C}$) but decreases during hydrate formation in frozen samples. Freezing and thawing of hydrate-bearing sediments above the equilibrium pressure reduces their thermal conductivity due to additional hydrate formation. On the other hand, thermal conductivity of hydrate-bearing frozen sediments may increase during dissociation of pore hydrates due to their self-preservation. It increases as the pore space contains smaller amounts of hydrates but more ice which is four times more thermally conductive.

Acknowledgements

This research is supported by the Russian Science Foundation (grant no. 16-17-00051).

Author details

Evgeny Chuvilin^{1,2*}, Boris Bukhanov¹, Viktor Cheverev², Rimma Motenko² and Erika Grechishcheva³

*Address all correspondence to: chuviline@msn.com

1 Skolkovo Institute of Science and Technology (Skoltech), Skolkovo Innovation Center, Moscow, Russia

2 Geology Faculty, Moscow State University (MSU), Moscow, Russia

3 OJSC Fundamentproekt, Moscow, Russia

References

- [1] Von-Herzen RP, Maxwell AE. The measurement of thermal conductivity of deep-sea sediments by a needle probe method. *Journal of Geophysical Research*. 1959;**84**:1629-1634
- [2] Ivanov NS, Gavriliev RI. *Thermal Properties of Frozen Rocks*. Nauka: Moscow; 1965. 74 pp. (in Russian)
- [3] Ivanov NS. *Heat and Mass Transfers in Frozen Rocks*. Novosibirsk: Nauka; 1969. 240 p. (in Russian)
- [4] Sass JH, Lachenbruch AH, Munroe RJ. Thermal conductivity of rocks from measurements on fragments and its application to heat-flow determinations. *Journal of Geophysical Research*. 1971;**76**(14):3391-3401
- [5] Farouki OT. *Thermal Properties of Soils*. CRREL: Hanover; 1981. 151 p
- [6] Balobaev VT, Pavlov AV, Perl'shtein GZ. *Thermal Study of Permafrost in Siberia*. Novosibirsk: Nauka; 1983. 214 p. (in Russian)
- [7] Blackwell DD, Steele JL. Thermal conductivity of sedimentary rocks: Measurement and significance. In: Naeser ND, McCulloch TH, editors. *Thermal History of Sedimentary Basins*. New York: Springer-Verlag; 1989. pp. 45-96
- [8] Clauser C, Huenges E. Thermal conductivity of rocks and minerals. In: Ahrens TJ, editor. *Rock Physics and Phase Relations: A handbook of physical constants*. Washington: American Geophysical Union; 1995. pp. 105-126
- [9] Beck AE. Methods for determining thermal conductivity and thermal diffusivity. In: Haenel R, Rybach L, Stegena L, editors. *Handbook of Terrestrial Heat-Flow Density Determination*. Dordrecht: Kluwer Academic Publisher; 1998. pp. 87-124
- [10] Gavriliev RI. *Thermal Properties of Rocks and Soils in Permafrost Regions*. Novosibirsk: SO RAN; 1998. 208 p. (in Russian)
- [11] Côté J, Konrad J-M. Thermal conductivity of base-course materials. *Canadian Geotechnical Journal*. 2005;**42**:61-78. DOI: 10.1139/T04-081
- [12] Côté J, Konrad J-M. A generalized thermal conductivity model for soils and construction materials. *Canadian Geotechnical Journal*. 2005;**42**:443-458. DOI: 10.1139/T04-106
- [13] Côté J, Grosjean V, Konrad J-M. Thermal conductivity of bitumen concrete. *Canadian Journal of Civil Engineering*. 2013;**40**:172-180. DOI: 10.1139/cjce-2012-0159
- [14] Penner E. Thermal conductivity of frozen soils. *Canadian Journal of Earth Sciences*. 1970;**7**:982-987
- [15] Ershov ED, Danilov ID, Cheverev VG. *Petrography of Frozen Soils*. Moscow: MSU; 1987. 311 p. (in Russian)

- [16] Williams PJ, Smith MW. *The Frozen Earth: Fundamentals of Geocryology*. Cambridge: Cambridge University Press; 1989. 306 p
- [17] Ershov ED, Komarov IA, Cheverev VG, Barkovskaya EN, Shesternev DM. Heat and mass transfer properties. In: Ershov ED, editor. *Fundamentals of Geocryology. Part 2. Lithogenetic Geocryology*. Moscow: MSU; 1996. pp. 118-133. (in Russian)
- [18] Motenko RG. Thermal properties and phase composition of frozen saline soils [PhD thesis] Moscow: MSU; 1997. 195 p. (in Russian)
- [19] Yershov ED. *General Geocryology*. Cambridge: Cambridge University Press; 1998. 580 p
- [20] Komarov IA. *Thermodynamics and Mass Transfer in Frozen Sediments*. Moscow: Nauchniy Mir; 2003. 608 p. (in Russian)
- [21] Cheverev VG. *The Nature of Cryogenic Properties of Soils*. Moscow: Nauchniy Mir; 2004. 234 p. (in Russian)
- [22] Sloan ED. *Clathrate Hydrates of Natural Gases*. 2nd ed. New York: Marcel Dekker; 1998. 757 p
- [23] Max MD, editor. *Natural Gas Hydrate in Oceanic and Permafrost Environments*. Boston: Kluwer Academic Publishers; 2000. 414 p
- [24] Cherskiy NV, Tsarev VP, Nikitin SP. Investigation and prediction of conditions of accumulation of gas resources in gas-hydrate pools. *Petroleum Geology*. 1985;**21**:65-89
- [25] Stoll RD, Bryan GM. Physical properties of sediments containing gas hydrates. *Journal of Geophysical Research*. 1979;**84**:1629-1634
- [26] Rosenbaum EJ, English NJ, Johnson JK, Shaw DW, Warzinski RP. Thermal conductivity of methane hydrate from experiment and molecular simulation. *The Journal of Physical Chemistry. B*. 2007;**111**:13193-13205
- [27] Waite WF, Stern LA, Kirby SH, Winters WJ, Mason DH. Simultaneous determination of thermal conductivity, thermal diffusivity and specific heat in sl methane hydrate. *Geophysical Journal International*. 2007;**169**:767-774
- [28] Andersland OB, Ladanyi B. *An Introduction to Frozen Ground Engineering*. Dordrecht: Springer-Science + Business Media; 1994. DOI: 10.1007/978-1-4757-2290-1
- [29] Muller SW. *Frozen in Time: Permafrost and Engineering Problems*. Virginia: ASCE; 2008. 280 p
- [30] Ye Y, Liu C. *Natural Gas Hydrates. Experimental Techniques and their Applications*. New York: Springer; 2013. 402 p
- [31] Warzinski RP, Gamwo IK, Rosenbaum EJ, Myshakin EM, Jiang H, Jordan KD, English NJ, Shaw DW. Thermal properties of methane hydrate by experiment and modeling and impacts upon technology. In: *Proceeding of the 6th International Conference on Gas Hydrates*; 6-10 July 2008; Vancouver; 2008
- [32] Popov Y, Beardsmore G, Clauser C, Roy S. ISRM suggested methods for determining thermal properties of rocks from laboratory tests at atmospheric pressure. *Rock Mechanics and Rock Engineering*. 2016;**49**:4179-4207. DOI: 10.1007/s00603-016-1070-5

- [33] Das BM. *Advanced Soil Mechanics*. 3rd ed. New York: Taylor & Francis; 2008. 567 p
- [34] Istomin V, Chuvilin E, Bukhanov B, Uchida T. Pore water content in equilibrium with ice or gas hydrate in sediments. *Cold Regions Science and Technology*. 2017;**137**:60-67. DOI: 10.1016/j.coldregions.2017.02.005
- [35] Grechishcheva E, Motenko R. Experimental study of freezing point and water phase composition of saline soils contaminated with hydrocarbons. In: *Proceedings of the 7th Canadian Permafrost Conference*; 21-23 September 2015; Quebec City; 2015: ABS_316
- [36] Roman LT. *Frozen Peat Soils as Foundations of Constructions*. Novosibirsk: Nauka; 1987. 222 p. (in Russian)
- [37] Groysman AG. *Thermal Properties of Gas Hydrates*. Novosibirsk: Nauka; 1985. 94 p. (in Russian)
- [38] Asher GB. *Development of computerized thermal conductivity measurement system utilizing the transient needle probe technique: An application to hydrates in porous media [PhD thesis]*. Colorado: Colorado School of Mines, Golden; 1987. 179 p
- [39] Huang D, Fan S. Measuring and modeling thermal conductivity of gas hydrate-bearing sand. *Journal of Geophysical Research*. 2005;**110**:B01311. DOI: 10.1029/2004JB003314
- [40] Duchkov AD, Manakov AY, Kazantsev SA, Permyakov ME, Ogienko AG. Thermal conductivity measurement of the synthetic samples of bottom sediments containing methane hydrates. *Izvestiya, Physics of the Solid Earth*. 2009;**45**:661-669. DOI: 10.1134/S1069351309080060
- [41] Yang L, Zhao J, Wang B, Liu W, Yang M, Song Y. Effective thermal conductivity of methane hydrate-bearing sediments: Experiments and correlations. *Fuel*. 2016;**179**:87-96. DOI: 10.1016/j.fuel.2016.03.075
- [42] Wright JF, Nixon FM, Dallimore SR, Hennings J, Cote MM. Thermal conductivity of sediments within the gas-hydrate-bearing interval at the JAPEX/JNOC/GSC et al. In: Dallimore SR, Collett TS, editors. *Mallik 5L-38 Gas Hydrate Production Research Well. Bulletin 585*. Ottawa: Geological Survey of Canada; 2005. pp. 1-5
- [43] Muraoka M, Ohtake M, Susuki N, Yamamoto Y, Suzuki K, Tsuji T. Thermal properties of methane hydrate-bearing sediments and surrounding mud recovered from Nankai trough wells. *Journal of Geophysical Research - Solid Earth*. 2014;**119**:8021-8033. DOI: 10.1002/2014JB011324
- [44] Muraoka M, Susuki N, Yamaguchi H, Tsuji T, Yamamoto Y. Thermal properties of a supercooled synthetic sand-water-gas-methane hydrate sample. *Energy & Fuels*. 2015; **29**(3):1345-1351. DOI: 10.1021/ef502350n
- [45] Chuvilin E, Bukhanov B. Effect of hydrate formation conditions on thermal conductivity of gas-saturated sediments. *Energy & Fuels*. 2017;**31**(5):5246-5254. DOI: 10.1021/acs.energyfuels.6b02726
- [46] Kuhs WF, Klapproth A, Gotthardt F, Techmer K, Heinrichs T. The formation of meso- and macroporous gas hydrates. *Geophysical Research Letters*. 2000;**27**(18):2929-2932

- [47] Staykova DK, Kuhs WF, Salamatin A, Hansen T. Formation of porous gas hydrates from ice powder: Diffraction experiments and multi-stage model. *Journal of Physical Chemistry B*. 2003;**107**:10299-10311
- [48] Bukhanov BA, Chuvilin EM, Guryeva OM, Kotov PI. Experimental study of the thermal conductivity of the frozen sediments containing gas hydrate. In: *Proceedings of the 9th International Conference on Permafrost (9-ICOP)*; 23 June-03 July 2008; Fairbanks; 2008. pp. 205-209
- [49] Chuvilin EM, Kozlova EV. Experimental estimation of hydrate-containing sediments stability. In: *Proceedings of the 5th International Conference on Gas Hydrate (ICGH-5)*; 12-16 June 2005; Trondheim; 2005. pp. 1540-1547
- [50] Chuvilin EM, Guryggeva OM. Experimental study of self-preservation effect of gas hydrates in frozen sediments. In: *Proceedings of the 9th International Conference on Permafrost (9-ICOP)*; 23 June-03 July 2008; Fairbanks; 2008. pp. 263-267
- [51] Hachikubo A, Takeya S, Chuvilin E, Istomin V. Preservation phenomena of methane hydrate in pore spaces. *Physical Chemistry Chemical Physics*. 2011;**13**:17449-17452. DOI: 10.1039/c1cp22353d
- [52] Takeya S, Fujihisa H, Gotoh Y, Istomin V, Chuvilin E, Sakagami H, Hachikubo A. Methane clathrate hydrates formed within hydrophilic and hydrophobic porous media: Kinetics of dissociation and distortion of host structure. *Journal of Physical Chemistry C*. 2013;**117**:7081-7085. DOI: 10.1021/jp312297h
- [53] Ershov ED, Lebedenko YP, Chuvilin EM, Yakushev VS. Experimental investigations of microstructure of ice—Methane hydrate agglomerate. *Engineering Geology*. 1990;**3**: 38-44 (in Russian)